

See discussions, stats, and author profiles for this publication at: <https://www.researchgate.net/publication/239377351>

Sol–Gel Cu–Al₂O₃ Adsorbents for Selective Adsorption of Thiophene out of Hydrocarbon

ARTICLE in INDUSTRIAL & ENGINEERING CHEMISTRY RESEARCH · AUGUST 2006

Impact Factor: 2.59 · DOI: 10.1021/ie060559t

CITATIONS

27

READS

47

5 AUTHORS, INCLUDING:



[Xiangxin Yang](#)

Kansas State University

12 PUBLICATIONS 472 CITATIONS

[SEE PROFILE](#)



[L. E. Erickson](#)

Kansas State University

306 PUBLICATIONS 4,277 CITATIONS

[SEE PROFILE](#)



[Keith L. Hohn](#)

Kansas State University

84 PUBLICATIONS 1,070 CITATIONS

[SEE PROFILE](#)



[Kenneth Klabunde](#)

Kansas State University

357 PUBLICATIONS 13,894 CITATIONS

[SEE PROFILE](#)

Sol–Gel Cu–Al₂O₃ Adsorbents for Selective Adsorption of Thiophene out of Hydrocarbon

Xiangxin Yang, Larry E. Erickson,* and Keith L. Hohn

Department of Chemical Engineering, Kansas State University, Manhattan, Kansas 66506

P. Jeevanandam and Kenneth J. Klabunde

Department of Chemistry, Kansas State University, Manhattan, Kansas 66506

The removal of thiophene from a hydrocarbon mixture by a novel Cu–Al₂O₃ adsorbent was investigated under ambient conditions. An adsorbent with 5 wt % Cu showed the highest capacity, 1.8 mg/g (milligram of sulfur per gram of adsorbent). A sol–gel process followed by supercritical drying, calcination, and thermovacuum treatment was successfully used to prepare the adsorbents. The adsorbents were characterized by Brunauer–Emmett–Teller specific surface area (BET), X-ray diffraction (XRD), and UV–vis diffuse reflectance spectroscopy (UV–vis). The characterization results suggested that copper ion with +1 valence was responsible for the adsorptive performance. Metallic copper (Cu⁰) and Cu²⁺ were not effective for the adsorption of thiophene. It seemed that Cu⁺ coordinated to thiophene through the sulfur atom, which was different from the mechanism of π -complexation proposed in the literature.

Introduction

Deep removal of sulfur from fuels has received more and more attention in research and development worldwide, not only because of health and environmental considerations but also due to the great need for producing ultralow-sulfur fuels.^{1,2} The SO_x pollutants produced during the combustion of transportation fuels are known precursors to acid rain. Also, sulfur in diesel fuel has a detrimental impact on the highly sulfur-sensitive advanced after-treatment strategies used to control the emission of nitrogen oxides (NO_x) and particulate matter (PM).^{3–5}

Fuel cells are believed to be one of the most promising and convenient energy conversion devices for generating electricity for both vehicles and stationary power plants because chemical energy can be converted directly into electrical energy with higher efficiency than in combustion engines.^{6,7} Gasoline and diesel fuel are ideal fuels for fuel cells due to their high energy density, ready availability, and proven safety for transportation and storage. However, organosulfur compounds contained in the fuels are poisonous to the catalysts used in reforming and water-gas-shift reactors in hydrocarbon-based fuel cell systems. It is generally accepted that sulfur content in the fuels must be reduced to less than 0.1 ppmw (parts per million by weight) for fuel cell application.^{8,9}

Traditionally, hydrosulfurization (HDS) with CoMo/Al₂O₃ or NiMo/Al₂O₃ catalysts and hydrogen has been used to remove sulfur from fuels by chemical reaction under high temperature (300–340 °C) and high pressure (20–100 atm of H₂).^{10,11} Reactivity of different sulfur compounds depends on the environment of the sulfur atom and the structure of the molecule. HDS is very efficient in removing thiols, sulfides, and disulfides because they have high electron density on the S atom and weaker C–S bond. But for thiophene and thiophene derivatives, HDS is less effective because of aromatic stabilization of the thiophene and benzothiophene rings.¹² Ultralow-sulfur specifications for fuels imply that the refractory sulfur compounds must be converted, which can be achieved under severe reaction

conditions with respect to pressure, temperature, and residence time, which significantly increases the cost of HDS. Consequently, development of new and affordable deep desulfurization processes for removing the refractory sulfur compounds is one of the major challenges for refineries and fuel cell research.

Several noncatalytic desulfurization technologies have been proposed in the literature. Rhodococcus was considered the most promising microbial biocatalyst, which could remove sulfur from substituted and unsubstituted dibenzothiophene (DBT) in the fuels, including sulfur compounds that hindered chemical catalysis and resisted removal by mild hydrotreatment.¹³ Oxidative desulfurization using hydrogen peroxide or ultrasound was reported by Filippis¹⁴ and Mei,¹⁵ where thiophenic compounds were oxidized to form sulfoxides and sulfones. One of the main advantages of the oxidative desulfurization process was that some sulfur compounds, which were among the most resistant to HDS due to their steric hindrance, showed a high reactivity toward oxidation. McKinley¹⁶ developed certain Ru(II) complexes, which in aqueous solution selectively bound and extracted 4,6-dimethyldibenzothiophene molecule from the hydrocarbon phase of simulated petroleum feedstock.

Desulfurization by adsorption is considered to be a promising and economical way to remove the less reactive sulfur compounds. The sulfur compounds are adsorbed by the solid adsorbents, and non-sulfur compounds are left untouched. From a technological point of view, adsorbents have to satisfy several requirements: selective adsorption of sulfur compounds, weak interaction between adsorbent and adsorbate for easy regeneration, and high capacity.¹⁷ A series of adsorbents based on the principle of π -complexation were reported by Yang and co-workers.^{2,9,18} The π -complexation bonds are stronger than van der Waals interactions, but they are also weak enough to be broken by moderate changes in temperature or pressure, providing the opportunity for selective adsorption of sulfur compounds from fuels. The authors found that Cu(I)–zeolite Y, Ag–zeolite Y, and CuCl/γ-Al₂O₃ were highly selective toward thiophene and their derivatives, and fuels with sulfur content less than 0.2 ppmw could be obtained. Song et al.^{1,6,7} proposed to remove sulfur from fuels over metal, metal sulfides,

* To whom correspondence should be addressed. Phone: 785-532-4313. Fax: 785-532-7372. E-mail: lerick@ksu.edu.

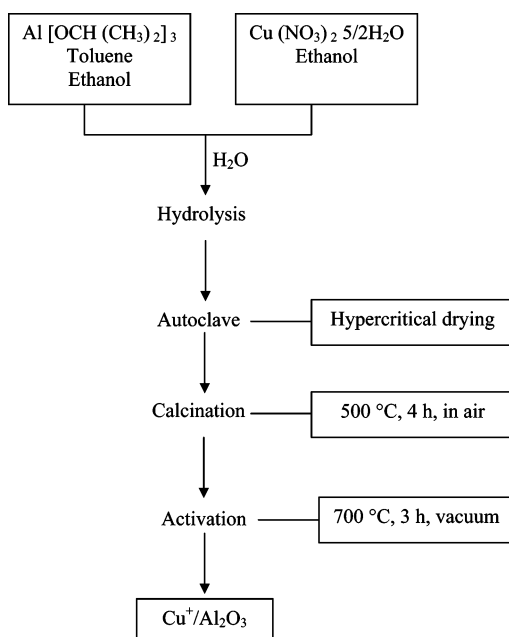


Figure 1. General procedure for preparation of adsorbents.

metal oxides, and zeolite-based adsorbents under ambient temperature and pressure. These adsorbents had been used to selectively remove sulfur from gasoline, diesel fuel, and jet fuel for producing ultraclean transportation fuels and for fuel-cell applications. Jeevanandam¹⁹ used nanocrystalline metal oxides as the adsorbents for desulfurization. Nanocrystalline metal oxides had several advantages: high surface area, open pore structure, and the loading level of metal ions (which was not limited by the charge compensation factors found in the case of zeolite). Adsorption of thiophene and benzothiophene in an organic model solution of hydrodesulfurized gasoline was studied by Xue¹⁰ using metal-ion-exchanged Y-zeolite adsorbents at 80 °C. Ce-Y-zeolite showed high adsorptive capacities for both sulfur compounds.

The sol-gel method is a technique for synthesis of materials with large surface area, low bulk density, uniform pore-size distribution, and good mechanical strength, which are particularly important to materials for separation applications.²⁰ The aim of this paper is to report the performance of sol-gel derived metal oxide adsorbents for desulfurization at ambient conditions and an in-depth study of the key factors that affect the adsorption.

Experimental Section

Preparation of Adsorbents. The Cu/Al₂O₃ adsorbents were prepared by the sol-gel/aerogel process using cupric nitrate and aluminum isopropoxide (98.0%, Aldrich). As shown in Figure 1, the general procedure for the preparation consisted of the following steps. An appropriate amount (0.076, 0.198, and 0.424 g corresponding to 2, 5, and 10 wt % of Cu, respectively) Cu(NO₃)₂·5/2H₂O was dissolved in 19 mL of ethanol. Aluminum isopropoxide (4.08 g) was put in a flask containing 133 mL of toluene and 60 mL of ethanol and stirred for 1 h. After complete dissolution, the Cu solution was added into the mixture. The hydrolysis was accomplished by adding about 2 mL of deionized water, followed by vigorous stirring at room temperature for 12 h. Afterward, an autoclave procedure was used to dry the gel under hypercritical conditions.²¹ After being flushed with a flow of N₂ gas, the Parr (autoclave) mini reactor was then pressurized with N₂ gas to obtain the initial pressure of 100

psi. The reactor was slowly heated from room temperature to 265 °C at a rate of 1 °C/min by PID controller. The overall heating time was about 4 h. The temperature was allowed to equilibrate at 265 °C for 15 min before the reactor was vented to release the pressure. The reactor was immediately removed from the heater and then flushed with N₂ for 10–15 min to remove any remaining organic solvent. During the heating, the pressure inside the reactor increased from 100 to 1000 psi. After it was allowed to cool to room temperature, the product was ground using an agate mortar. The powder was calcined at 500 °C for 4 h in air. The final activation step was conducted at 700 °C under vacuum for 3 h to promote autoreduction of Cu²⁺ to Cu⁺.

Characterization of Adsorbent. The specific surface area, pore volume, and average pore size of the samples were estimated using the N₂ adsorption-desorption isotherm at −196 °C by the multipoint Brunauer-Emmet-Teller (BET) method using a NOVA 1000 adsorption instrument (Quantachrome, USA). Before adsorption, all the samples were degassed for 1 h at 150 °C under vacuum. The surface area and pore volume were calculated using the adsorption isotherms. The desorption isotherms were used to calculate pore size distributions.

X-ray powder diffraction (XRD) patterns were obtained with a Bruker D8 diffractometer, using Cu Kα radiation (1.5406 Å) at 40 kV and 40 mA and a secondary graphite monochromator. The measurements were recorded in steps of 0.025° with a count time of 1 s in the 2θ range of 20–80°. Identification of the phases was made with the help of the Joint Committee on Powder Diffraction Standards (JCPDS) files.

UV-visible spectra (UV-vis) measurements were carried out on a Cary 500 spectrophotometer equipped with a Cary 4/5 diffuse reflection sphere, in the 200–800 nm wavelength range. The baseline was recorded using a poly(tetrafluoroethylene) reference. All spectra were taken under atmospheric conditions.

Adsorption Experiments. Adsorption experiments were performed by a batch method. After the activation, the adsorbent was quickly mixed with 40 mL of model fuel consisting of pentane and thiophene (the S level of the model fuel is 20 ppmw). The mixture was kept in a sealed tube at room temperature with stirring for a desired time. The liquid phase was separated from the adsorbent, and the sulfur concentration in the solution was monitored by UV-vis spectrophotometry (thiophene has an absorption band at about 230 nm and the absorbance corresponds to the residual thiophene content).

Results and Discussion

Figure 2 shows thiophene adsorption results on Cu/Al₂O₃ adsorbents with different loadings. In this figure, the smallest absorbance means the largest amount of thiophene was adsorbed. The adsorbent with 5 wt % Cu showed the highest capacity, 1.8 mg/g. The sulfur content of the solution after adsorption was 2.0 ppmw. The capacities were 1.5 and 0.9 mg/g for 2 and 10 wt % Cu adsorbents, respectively. The corresponding sulfur contents were 5 and 11 ppmw for the remaining solutions. It was clear that sol-gel prepared Cu/Al₂O₃ held considerable promise for thiophene adsorption.

Figure 3 shows the kinetics of thiophene adsorption on the 5 wt % Cu/Al₂O₃ adsorbent. The adsorption was very fast during the first 30 min, and equilibrium was nearly achieved after 1.5 h.

Morphology of the Cu/Al₂O₃ Adsorbents. The adsorption/desorption isotherms for various adsorbents were typical of type IV, which was characteristic of mesoporous solids.²² Quantitative comparisons on the pore structure of various samples are

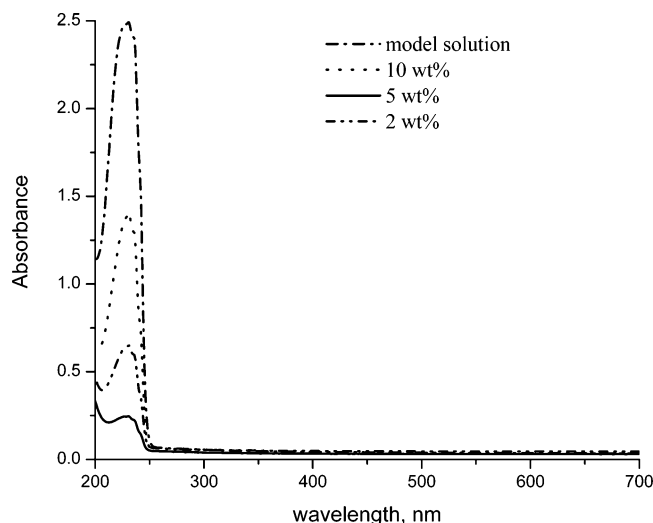


Figure 2. Adsorption of thiophene on Cu/Al₂O₃ with different Cu loadings.

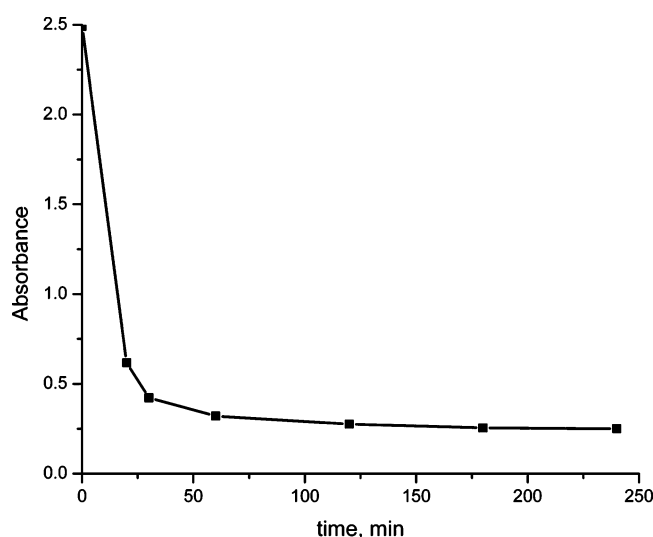


Figure 3. Kinetics of thiophene adsorption on 5 wt % Cu/Al₂O₃ adsorbent.

Table 1. Pore Structure of Cu/Al₂O₃ Adsorbents

adsorbents	surface area (m ² /g)	pore volume (cm ³ /g)	pore diameter (nm)
0 wt % Cu/Al ₂ O ₃	452	2.1	17
2 wt % Cu/Al ₂ O ₃	425	1.9	16
5 wt % Cu/Al ₂ O ₃	385	1.9	12
10 wt % Cu/Al ₂ O ₃	357	1.5	5

reported in Table 1. The copper loading had a great influence on the textural properties. The BET surface area, pore volume, and pore diameter did not change with lower loading, showing that the structure of the support was preserved. The small decrease of these parameters was attributed to plugging by very fine crystallites of CuO. At higher loading, the insertion of copper decreased the pore diameter greatly, which was presumably the result of blockage of some pores by CuO particles as shown later by XRD results.

XRD. Figure 4 shows XRD patterns of the Cu/Al₂O₃ samples before calcination, after calcination, and after thermovacuum treatment. Metallic copper diffraction lines were observed for the samples before calcination treatment, indicating that much of the Cu²⁺ was reduced during the hypercritical drying step. The intensity of the XRD peaks due to copper increased as the copper content increased. After calcination at 500 °C, no peaks due to copper species were observed for samples with less than 5 wt % copper loading, suggesting that copper was highly

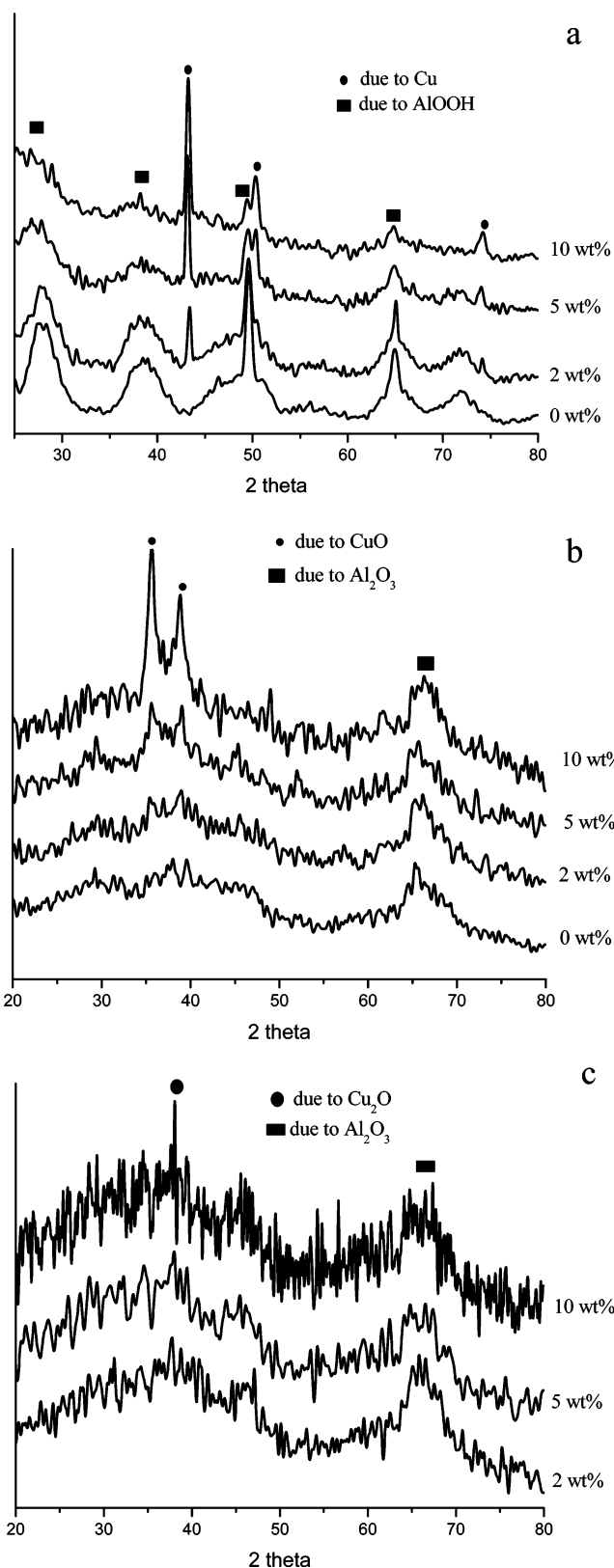


Figure 4. XRD patterns of Cu/Al₂O₃ adsorbents with different Cu loadings (a) before calcination, (b) after calcination, and (c) after thermovacuum treatment.

dispersed on the support surface or the crystallite size of the copper species was so small that they were undetectable as a consequence of sensitivity and size limits of the XRD technique. Weak diffraction lines of crystalline CuO ($2\theta = 35.5$ and 38.7°) were confirmed on 5 wt % Cu/Al₂O₃. More intensive diffraction lines were noticed for 10 wt % Cu/Al₂O₃. This showed that the

bulk structure of samples with low copper content was rather similar to that of alumina, which had a defective spinel phase with low crystallinity.²³ Autoreduction of Cu^{2+} to Cu^+ after thermovacuum treatment was confirmed by the Cu_2O diffraction lines observed for 10 wt % $\text{Cu}/\text{Al}_2\text{O}_3$. The lack of Cu_2O peaks in the lower copper loading samples was also attributed to the small crystal size of Cu_2O or the limit of XRD. Compared with the black color observed in $\text{Cu(II)}/\text{Al}_2\text{O}_3$ (calcined samples), the color of $\text{Cu(I)}/\text{Al}_2\text{O}_3$ (after thermovacuum treatment) was light gray, which was also evidence of autoreduction;²⁴ Cu(I) species are usually colorless except where color results from charge transfer to the anion.²⁵ The mechanism of thermal reduction of Cu^{2+} was assumed as follows: the coordinated hydroxyl groups of the isolated Cu^{2+} ions were desorbed as water during calcination. The evolution of two oxygen ligands as an oxygen molecule from the dehydrated Cu^{2+} monomer caused the thermal reduction of Cu^{2+} into the low-coordinated Cu^+ ion.²⁶

UV–Vis. Figure 5 shows the diffuse reflectance UV–vis spectra of $\text{Cu–Al}_2\text{O}_3$ samples before calcination, after calcination, and after thermovacuum treatment. According to literature, the strong absorption between 200 and 300 nm were due to the LMCT (ligand to metal charge transfer) band of Cu^{2+} species. Absorption between 600 and 800 nm corresponded to the d–d transition band of Cu^{2+} situated in an octahedral O_h configuration more or less tetragonally distorted. Fine Cu metallic particles exhibited absorption in the 580–590 nm range corresponding to the conduction band.^{27,28,29}

Before calcination, absorption bands in the spectrum of the sample without copper (support) were observed at 210 and 270 nm. This might be due to trace impurities in the aluminum isopropoxide. A small peak in this region assigned to a LMCT transition from oxygen to contaminant transition metal cations was previously reported by Yamamoto.²⁸ For samples with copper, we could not rule out the existence of Cu^{2+} species because the LMCT absorption band of Cu^{2+} species overlapped with that of contaminant of the support in the region of 200–300 nm. Also, another band around 600 nm was observed, showing that Cu^{2+} was reduced to Cu^0 during the hypercritical drying process, which was in good agreement with XRD results.

After calcination, the diffuse reflectance spectra showed strong absorption bands at 240 nm and a broad absorption from 350 to 800 nm. The band at 240 nm might be the LMCT band. We assigned the broad absorption to CuO or bulklike spinel CuAl_2O_4 species because both showed absorption in this range. The three-dimensional Cu^+ cluster in the CuO matrix was also reported to show some absorption in this range (400–500 nm).³⁰ Since the samples were calcined and the spectra measured in air, the existence of Cu^+ species was less likely. With the increase of copper loading, the LMCT band shifted to the higher wavelength and the intensity increased, indicating the less tetragonal distortion of the copper species in the octahedral environment.³⁰ The intensity of the absorption in the 350–800 nm range increased, and the strong absorption band between 200 and 300 nm decreased when copper loading increased from 5 to 10 wt %, showing the increase of crystalline and bulk CuO .²⁷ This was consistent with the observation that the intensities of the XRD peaks increased with the increase of copper loading. The absorption band at 270 nm in the spectrum of the support was also due to metal oxide impurities.

After the thermovacuum treatment, a new absorption band appeared at 320 nm, which was assigned to the electron transition $d^{10} \rightarrow d^9s^1$ of Cu^+ species (Cu_2O). Although the 3d orbitals of Cu_2O were fully occupied and no d–d transition band

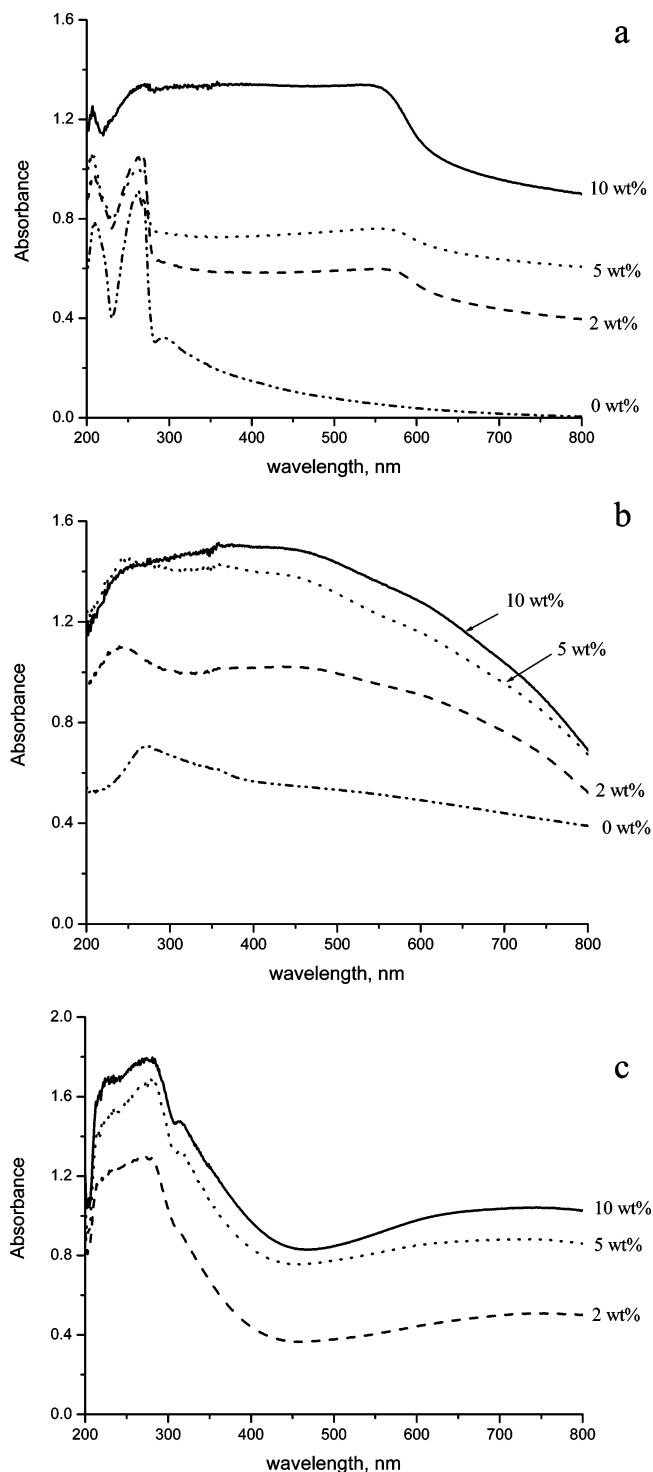


Figure 5. Diffuse reflectance UV–vis spectra of $\text{Cu}/\text{Al}_2\text{O}_3$ adsorbents with different Cu loadings (a) before calcination, (b) after calcination, and (c) after thermovacuum treatment.

should be observed, Cu_2O could give transitions from the valence band to excited levels involving the emission and absorption of a photon.³⁰ The appearance of Cu_2O was also observed by XRD. It was obvious that reduction ($\text{Cu}^{2+} \rightarrow \text{Cu}^+$) was not complete from the UV–vis spectra because there still existed a Cu^{2+} species absorption band after thermovacuum treatment. The degree of the Cu^{2+} dispersion determined the autoreducibility. The isolated Cu^{2+} ions were more easily reduced to Cu^+ in a vacuum.²⁶ This was in good agreement with the results of our adsorption experiments. For adsorbents with copper loadings of 2 and 5 wt %, copper ions were highly

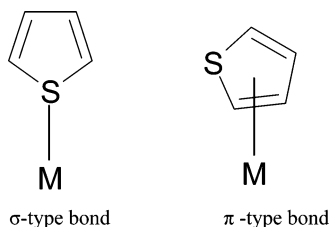


Figure 6. Two possible interactions between thiophene and metal ion.

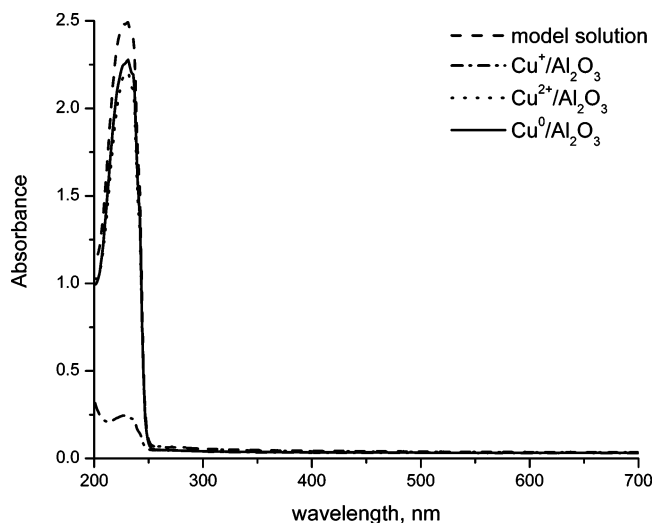


Figure 7. Adsorption of thiophene on 5 wt % Cu/Al₂O₃ adsorbent with different Cu oxidation states.

dispersed and easy to reduce in a vacuum. The 5 wt % Cu/Al₂O₃ adsorbent showed higher capacity. More aggregates were formed in the case of 10 wt % Cu/Al₂O₃, and Cu²⁺ ions were more difficult to reduce, so capacity was also lower. At the present time, we are not able to quantify the percentage of reduced copper.

Mechanism of Adsorption. Although mechanistic research has been carried out by experiments and simulations, debate continues over the role of metal ions and the identity of the active sites. Thiophene has two lone pairs of electrons on the sulfur atom; one pair lies on the six-electron system and the other lies in the plane of the ring. Thiophene can act either as an n-type donor by donating the lone pair of electrons (direct S–M σ bond) or as π -type donor by unitizing the delocalized electrons of the aromatic ring (π bond) to form π -type complex with the metal ions (Figure 6).¹⁰ On the basis of the molecular orbital theory calculation, Yang et al.^{2,9,18} suggested the π -complexation mechanism. In this mechanism, the cations can form the usual σ bonds with their s orbitals and, in addition, their d orbitals back-donate electron density to the antibonding π orbitals of the sulfur rings. Song et al.^{1,6,7} reported that there existed a direct interaction between the metal atom and sulfur atom of the thiophenic molecules, known to be possible with some organometallic complexes. Among the known coordination geometries of thiophene in organometallic complexes, only two types of interaction of thiophene with metal involved sulfur in thiophene (the sulfur atom interacted with one metal atom or two metal atoms).

Figure 7 shows the thiophene adsorption results of three adsorbents: Cu⁰/Al₂O₃ (no calcination, heating in a vacuum), Cu²⁺/Al₂O₃ (calcination, heating in air), and Cu⁺/Al₂O₃ (calcination, heating in a vacuum). All three adsorbents had 5 wt % copper loading. Both Cu²⁺ and Cu⁰ were ineffective for

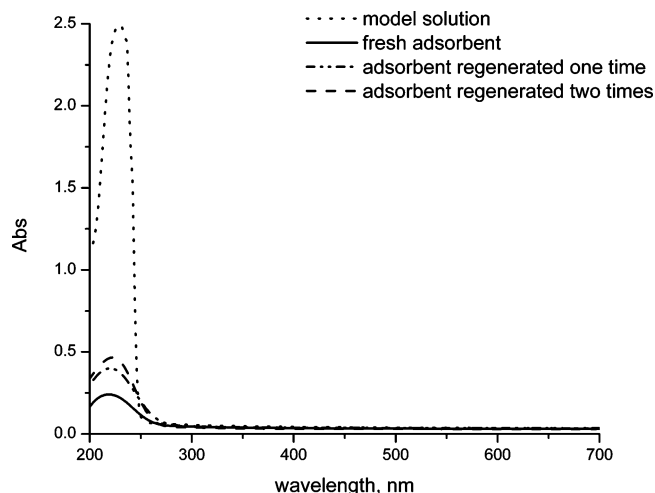


Figure 8. Adsorption of thiophene on fresh and regenerated 5 wt % Cu/Al₂O₃ adsorbent.

thiophene removal. Only Cu⁺ showed high adsorption capacity toward thiophene. The π -complexation mechanism suggests that Cu⁰ could selectively bind to the π -system of thiophene and remove it; however, our data do not support this expectation. The inconsistency might be due to the preparation methods, supports, pretreatments, or the interactions among the coexisting molecules in the fuel. It appears that thiophene coordinated to the metal ion (Cu⁺) through its sulfur atom in our experiments, but it has not been proven at this point. Based on the difference of NMR chemical shifts between the DBT in the AgBF₄–DBT solution and those of the free DBT, McKinley³¹ found that DBT coordinated to Ag⁺ through the sulfur atom instead of the arene ring.

Regeneration of Adsorbent. The regeneration of adsorbents after adsorption was studied by heating the adsorbent in a vacuum (700 °C, 3 h) to remove the adsorbed sulfur compounds and to reduce Cu²⁺ to Cu⁺, using 5 wt % Cu/Al₂O₃ adsorbent. In Figure 8, the effect of regeneration on adsorption was illustrated. The thiophene uptake reached more than 95% when the adsorption equilibrium was attained. Even after the second regeneration, the adsorption capacity was 1.7 mg/g, 95% of the capacity of the fresh adsorbent. Thus, the adsorbent could be easily regenerated without losing its capacity.

Conclusions

Sol–gel prepared Cu/Al₂O₃ adsorbents were effective in the removal of thiophene from a hydrocarbon liquid. The adsorption experiments, along with characterization results suggested that Cu²⁺ and Cu⁰ did not adsorb thiophene; Cu⁺ was the active adsorption site. The kinetic study suggested that the adsorption equilibrium was attained after 1.5 h and most of the adsorption occurred in the first 30 min. The adsorbents had good regenerative properties; 95% of the capacity remains after two adsorption cycles. Future work will investigate the mechanism further, test different sol–gel materials for their thiophene adsorption capacities, and evaluate the adsorbents for desulfurization of real fuels.

Literature Cited

- (1) Song, C. S. An Overview of New Approaches to Deep Desulfurization for Ultra-Clean Gasoline, Diesel Fuel and Jet Fuel. *Catal. Today* **2003**, *86*, 211.
- (2) Hernandez-Maldonado, A. J.; Yang, R. T. Desulfurization of Transportation Fuels by Adsorption. *Catal. Rev.* **2004**, *46*, 111.

- (3) Diesel Emission Controls Sulfur Effects (DECSE) Program, Final Report: Diesel Oxidation Catalysts and Lean-NO_x Catalysts, June 2001. <http://www.ott.doe.gov/decse/pdfs/decserpt.pdf>.
- (4) Ninth Report on Carcinogens 2000. <http://ntp.niehs.nih.gov/ntp/roc/eleventh/profiles/s069dies.pdf>.
- (5) Boehman, A. L.; Song, J. H.; Alam, M. Impact of Biodiesel Blending on Diesel Soot and the Regeneration of Particulate Filters. *Energy Fuels* **2005**, *19*, 1857.
- (6) Ma, X. L.; Sprague, M.; Song, C. S. Deep Desulfurization of Gasoline by Selective Adsorption over Nickel-Based Adsorbent for Fuel Cell Applications. *Ind. Eng. Chem. Res.* **2005**, *44*, 5768.
- (7) Ma, X. L.; Sun, L.; Song, C. S. A New Approach to Deep Desulfurization of Gasoline, Diesel Fuel and Jet Fuel by Selective Adsorption for Ultra-Clean Fuels and for Fuel Cell Applications. *Catal Today* **2002**, *77*, 107.
- (8) Jayne, D.; Zhang, Y.; Haji, S.; Erkey, C. Dynamics of Removal of Organosulfur Compounds from Diesel By Adsorption on Carbon Aerogels for Fuel Cell Application. *Int. J. Hydrogen Energy* **2005**, *30*, 1287.
- (9) Hernandez-Maldonado, A. J.; Yang, R. T. New Sorbents for Desulfurization of Diesel Fuels via π -Complexation. *AIChE J.* **2004**, *50* (4), 791.
- (10) Xue, M.; Chitrakar, R.; Skane, K. Selective Adsorption of Thiophene and 1-Benzothiophene on Metal-Ion-Exchanged Zeolite in Organic Medium. *J. Colloid Interface Sci.* **2005**, *285*, 487.
- (11) Gates, B. C.; Katzer, J. R.; Schuit, G. C. *Chemistry of Catalytic Processes*; McGraw-Hill: New York, 1979; p 390.
- (12) Reynolds, M. A.; Guzei, I. A.; Angelici, R. J. Re(CO)₁₀-Mediated Carbon-Hydrogen and Carbon-Sulfur Bond Cleavage of Dibenzothiophene and 2,5-Dimethylthiophene. *Organometallics* **2001**, *20*, 1071.
- (13) McFarland, B. L.; Boron, D. J.; Deever, W.; Meyer, J. A.; Johnson, A. R.; Atlas, R. M. Biocatalytic Sulfur Removal from Fuels: Applicability for Producing Low Sulfur Gasoline. *Crit. Rev. Microbiol.* **1998**, *24* (2), 99.
- (14) Filippis, P. D.; Scarsella, M. Oxidative Desulfurization: Oxidation Reactivity of Sulfur Compounds in Different Organic Matrixes. *Energy Fuels* **2003**, *17*, 1452.
- (15) Mei, H.; Mei, B. W.; Yen, T. F. A New Method for Obtaining Ultra-low Sulfur Diesel Fuel via Ultrasound Assisted Oxidative Desulfurization. *Fuel* **2003**, *82* (4), 405.
- (16) McKinley, S. G.; Angelici, R. J. Extraction of Dibenzothiophenes from Petroleum Feedstocks Using a Ruthenium Complex in Aqueous Solution. *Energy Fuels* **2003**, *17*, 1480.
- (17) Richardeau, D.; Joly, G.; Canaff, C. Adsorption and Reaction over HFAU Zeolites of Thiophene in Liquid Hydrocarbon Solutions. *Appl. Catal., A* **2004**, *263*, 49.
- (18) Yang, R. T. *Adsorbents: Fundamentals and Applications*; Wiley: New York, 2003; p 280.
- (19) Jeevanandam, P.; Klabunde, K. J.; Tetzler, S. H. Adsorption of Thiophenes out of Hydrocarbons Using Metal Impregnated Nanocrystalline Aluminum Oxide. *Microporous Mesoporous Mater.* **2005**, *79*, 101.
- (20) Deng, S. G.; Lin, Y. S. Sol-Gel Preparation and Properties of Alumina Adsorbents for Gas Separation. *AIChE J.* **1995**, *41* (3), 559.
- (21) Utamapanya, S.; Klabunde, K. J.; Schlup, J. R. Nanoscale Metal Oxide Particles/Clusters as Chemical Area Magnesium Hydroxide and Magnesium Oxide Reagents. Synthesis and Properties of Ultrahigh Surface. *Chem. Mater.* **1991**, *3*, 175.
- (22) Zhu, Z. H.; Zhu, H. Y.; Wang, S. B.; Lu, G. Q. Preparation and Characterization of Copper Catalysts Supported on Mesoporous Al₂O₃ Nanofibers for N₂O Reduction to N₂. *Catalysis Lett.* **2003**, *91*(1–2), 73.
- (23) Shimizu, K.; Maeshima, H.; Yoshida, H. Spectroscopic Characterisation of Cu–Al₂O₃ Catalysts for Selective Catalytic Reduction of NO with Propene. *Phys. Chem. Chem. Phys.* **2000**, *2*, 2435.
- (24) Hernandez-Maldonado, A. J.; Yang, R. T. Desulfurization of Liquid Fuels by Adsorption via π Complexation with Cu(I)–Y and Ag–Y Zeolites. *Ind. Eng. Chem. Res.* **2003**, *42*, 123.
- (25) <http://wwwchem.uwimona.edu.jm:1104/courses/copper.html>.
- (26) Amano, F.; Tanaka, T.; Funabiki, T. Auto-reduction of Cu(II) Species Supported on Al₂O₃ to Cu(I) by Thermovacuum Treatment. *J. Mol. Catal. A: Chem.* **2004**, *221*, 89.
- (27) Chary, K. V. R.; Sagar, G. V.; Naresh, D.; Seela, K. K.; Sridhar, B. Characterization and Reactivity of Copper Oxide Catalysts Supported on TiO₂–ZrO₂. *J. Phys. Chem. B* **2005**, *109*, 9437.
- (28) Yamamoto, T.; Tanaka, T.; Kuma, R.; Suzuki, S.; Amano, F.; Shimooka, Y.; Kohno, Y.; Funabiki, T.; Yoshida, S. NO Reduction with CO in the Presence of O₂ over Al₂O₃-Supported and Cu-Based Catalysts. *Phys. Chem. Chem. Phys.* **2002**, *4*, 2449.
- (29) Chen, L. Y.; Horiuchi, T. Catalytic Selective Reduction of NO with Propylene over Cu–Al₂O₃ Catalysts: Influence of Catalyst Preparation Method. *Appl. Catal., B* **1999**, *23*, 259.
- (30) Praliaud, H.; Mikhalienco, S.; Chajar, Z.; Primet, M. Surface and Bulk Properties of Cu–ZSM-5 and Cu/Al₂O₃ Solids During Redox Treatments: Correlation with the Selective Reduction of Nitric Oxide by Hydrocarbons. *Appl. Catal., B* **1998**, *16*, 359.
- (31) McKinley, S. G.; Angelici, R. J. Deep Desulfurization by Selective Adsorption of Dibenzothiophene on Ag⁺/SBA-15 and Ag⁺/SiO₂. *Chem. Commun.* **2003**, 2620.

Received for review May 3, 2006

Revised manuscript received July 7, 2006

Accepted July 11, 2006

IE060559T